Original Article

Comparison of autologous ^{111}In-leukocytes, ^{18}F-FDG, ^{11}C-methionine, ^{11}C-PK11195 and ^{68}Ga-citrate for diagnostic nuclear imaging in a juvenile porcine haematogenous *staphylococcus aureus* osteomyelitis model

Ole L Nielsen[1], Pia Afzelius[2], Dirk Bender[3], Henrik C Schønheyder[4,5], Páll S Leifsson[1], Karin M Nielsen[1,6], Jytte O Larsen[7], Svend B Jensen[6,8*], Aage KO Alstrup[3*]

*[1]Department of Veterinary Disease Biology, University of Copenhagen, Copenhagen; [2]Department of Diagnostic Imaging, North Zealand Hospital, Hillerød; [3]Department of Nuclear Medicine and PET Centre, Aarhus University Hospital, Aarhus; [4]Department of Clinical Microbiology, Aalborg University Hospital, Aalborg; [5]Department of Clinical Medicine, Aalborg University, Aalborg; [6]Department of Nuclear Medicine, Aalborg University Hospital, Aalborg, [7]Department of Neuroscience and Pharmacology, University of Copenhagen, Copenhagen; [8]Department of Chemistry and Biochemistry, Aalborg University, Aalborg, Denmark. *Joint senior co-authorship.*

Abstract: The aim of this study was to compare ^{111}In-labeled leukocyte single-photon emission computed tomography (SPECT) and ^{18}F-fluorodeoxyglucose (^{18}F-FDG) positron emission tomography (PET) to PET with tracers that potentially could improve detection of osteomyelitis. We chose ^{11}C-methionine, ^{11}C-PK11195 and ^{68}Ga-citrate and validated their diagnostic utility in a porcine haematogenous osteomyelitis model. Four juvenile 14-15 weeks old female pigs were scanned seven days after intra-arterial inoculation in the right femoral artery with a porcine strain of *Staphylococcus aureus* using a sequential scan protocol with ^{18}F-FDG, ^{68}Ga-citrate, ^{11}C-methionine, ^{11}C-PK11195, ^{99m}Tc-Nanocoll and ^{111}In-labelled autologous leukocytes. This was followed by necropsy of the pigs and gross pathology, histopathology and microbial examination. The pigs developed a total of five osteomyelitis lesions, five lesions characterized as abscesses/cellulitis, arthritis in three joints and five enlarged lymph nodes. None of the tracers accumulated in joints with arthritis. By comparing the 10 infectious lesions, ^{18}F-FDG accumulated in nine, ^{111}In-leukocytes in eight, ^{11}C-methionine in six, ^{68}Ga-citrate in four and ^{11}C-PK11195 accumulated in only one lesion. Overall, ^{18}F-FDG PET was superior to ^{111}In-leukocyte SPECT in marking infectious and proliferative, i.e. hyperplastic, lesions. However, leukocyte SPECT was performed as early scans, approximately 6 h after injection of the leukocytes, to match the requirements of the 18 h long scan protocol. ^{11}C-methionine and possibly ^{68}Ga-citrate may be useful for diagnosis of soft issue lesions.

Keywords: Osteomyelitis, models, animal, domestic pigs, *sus scrofa*, swine, *staphylococcus aureus*, positron-emission tomography, tomography, emission-computed, single-photon, tomography, X-Ray computed, Inflammation, Infection

Introduction

Osteomyelitis in humans is primarily caused by *Staphylococcus aureus* regardless of gender, age, anatomical region and place of acquisition [1, 2]. The origin is either haematogenous, induced by contiguous inoculation (including infection following trauma or e.g. joint replacement) or appears secondary to vascular insufficiency in people with e.g. diabetes [3].

In adults, osteomyelitis is often associated with bone surgery and joint replacement, but can also localize to the axial skeleton by the haematogenous route. The diagnostic imaging techniques include computed tomography (CT), leukocyte scintigraphy, bone scintigraphy, bone marrow scintigraphy and ^{18}F-FDG PET [4, 5].

In contrast, the majority of cases of osteomyelitis in children are haematogenous, and the

infection tends to localize in zones of growth in the long bones [2]. Here diagnostic imaging mainly relies on plain radiographs, magnetic resonance imaging (MRI), and bone scintigraphy [6-8].

A haematogenous *S. aureus* osteomyelitis model using juvenile pigs was recently developed and characterized [9, 10]. On one side, the femoral artery was inoculated with *S. aureus*, and subsequently osteomyelitis lesions developed exclusively in that limb with insignificant signs of further spread. Also, the pigs developed only mild clinical signs, and the model seemed to be highly discriminatory for osteomyelitis in children.

The aim of the present study was to compare the traditional inflammation imaging protocols of labeled leukocyte SPECT and ^{18}F-FDG PET to PET tracers less well characterized for the visualization of inflammation using the porcine juvenile osteomyelitis model. We chose to include ^{11}C-methionine, ^{11}C-PK11195 and ^{68}Ga-citrate. ^{11}C-methionine is a radiolabelled amino acid tracer which will image amino acid metabolism. Although methionine accumulates in inflammatory lesions, it is primarily used as a marker of malignancies with an ability to distinguish these from both suppurative and granulomatous inflammatory lesions at least in rats [11]. The uptake is relatively low in extremities of children and young adults and may thus be suitable for indicating lesions in the limbs [12]. ^{11}C-PK11195 is a specific ligand of the peripheral benzodiazepine receptor highly expressed on activated mononuclear phagocytic cells and has previously been used to diagnose neuroinflammation. It has also been used in an attempt to visualize inflammation at other anatomical sites, e.g. in macrophage-dominated blood vessels and tissue membranes surrounding loosening prostheses in rat models [13-15]. ^{67}Ga-citrate SPECT has been used widely to aid the diagnosis of bone infections. Gallium ions binds to lactoferrin present in high concentrations in neutrophils and abscess fluid, and binds to siderophores produced by microorganisms [16]. However, suitable images can be obtained only after 24-72 h, and the sensitivity, specificity and resolution are low due to substantial background uptake [4, 17]. In recent years, the interest has shifted towards use of the short lived positron-emitting radionuclide ^{68}Ga as a marker of bone infection and infection in general, because of the improved image quality of PET technology, high resolution, reduced radiation exposure and the possibility of completing the diagnostic procedures within one to two h [18, 19].

We hypothesize that the osteomyelitis model is feasible for testing and comparing various SPECT and PET tracers, and that one or more of the PET tracers may prove superior to the time-consuming and potential hazardous autologous leukocyte labeling and SPECT.

Material and methods

Pigs

The study was conducted in four rounds with two pigs per round, using clinically healthy, female, specific pathogen-free (SPF), Danish landrace cross-breed pigs reared for meat production. The pigs were purchased from a local commercial pig farmer and upon arrival at the experimental animal facility (Paaskehøjgaard, Aarhus University), the two pigs (aged 12-13 weeks) were housed in separate pens, fed twice daily with restricted pellet diet (DIA plus FI, DLG, Denmark) and had *ad libitum* access to tap water. The pigs remained clinically healthy during the acclimatization period of 8 days, during which venous blood samples were obtained for haematology and measurements of acute phase proteins. The study was approved by the Danish Animal Experimentation Board, journal no. 2012-15-2934-000123, and the humane endpoints for immediate euthanasia were: clinical signs of systemic infection (fever for more than 24 h, shallow respiration), anorexia or reluctance to drink for more than 24 h, more than 10% loss of bodyweight (bw), pain that was untreatable with opioid analgesics, or refusal to stand up. All facilities were approved by the Danish Occupational Health Surveillance.

Microbiology

The inoculum was prepared from the S54F9 strain of *S. aureus* (spa type t1333, MLST sequence type ST433 and clonal complex CC30), isolated from a chronic embolic pulmonary abscess in a pig [20-22]. Overnight cultures on 5% horse blood agar (HBA) (SSI Diagnostica, Denmark) were harvested, suspended in 0.9% sterile saline and adjusted to McFarlane 0.5. The target inoculum was pre-

pared by serial dilution and numbers of colony forming units (CFUs) as well as purity were determined by plating aliquots on 5% HBA with incubation overnight at 35°C.

Tissue specimens and swabs obtained at necropsy were plated on 5% HBA and read after incubation overnight. *S. aureus* was confirmed by latex agglutination (Monostaph Plus, Bionor Laboratories, Norway). Growth characteristics including a pansusceptible antibiogram were taken to indicate identity with the inoculated strain. Contaminants were sparse and characterized primarily by Gram stain. A few isolates were identified to species level by matrix-assisted laser desorption/ionization-time of flight (MALDI-TOF) (Bruker Daltonik GmbH, Bremen, Germany).

The pig osteomyelitis model

Inoculation was done into the right femoral artery, using the technique described by Johansen et al. [9, 10]. Briefly, the pigs were sedated with intramuscular (im) injections of 5 mg/kg bw azaperone (Stressnil, Eli Lilly, Hampshire, England) and 0.6 mg/kg bw midazolam (Midazolam Hameln, Hameln Pharmaceuticals, Hameln, Germany) and anaesthetized by intravenous (iv) pump infusion of 5-10 mg/h/kg bw propofol (Propofol Braun, B. Braun Melsungen AG, Melsungen, Germany) through a catheter placed in the ear vein. Forced ventilation (270 mL/min, frequency of 15/min) and monitoring of oxygen saturation and heart rate were achieved by endotracheal intubation and using a respirator-and-monitor system (Dräger Julian, Dräger Medizintechnik, Lübeck, Germany). An intra-arterial catheter mounted with a three way stop was placed through a skin incision into the blood-empty (proximally clamped) right femoral artery, with the tip of the catheter pointing distally. Inocula ranging from 10,500 to 141,000 CFU/kg bw suspended in 1.0 to 3.5 mL of sterile saline were injected intra-arterially into the eight pigs. This was followed by removal of the catheter and either continued clamping for 10 min combined with an additional 10 min manual arterial compression after the clamp had been removed, or only removal of the clamp and then 10 min of manual compression. Finally, the wound was sutured. After inoculation and recovery from anaesthesia, the pigs were monitored extensively clinically the following days, and signs of disease were noted.

After clinical signs had occurred or no later than 7 days after inoculation, i.e. the day of scan, post inoculation (pi) venous blood samples were obtained for haematology and measurements of acute phase proteins; measurement of blood glucose was performed on the day of scan, as was the bw. Buprenorphine (Temgesic, Reckitt Benckiser, Berkshire, England) was given to all pigs during surgery and from day 3-4 and onwards, 0.3-0.9 mg im.

Haematology and acute phase proteins

Haematology was performed by the Central Laboratory, Department of Veterinary Clinical and Animal Sciences, Faculty of Health and Medical Sciences, University of Copenhagen, Copenhagen. An automated complete blood cell count including a leukocyte differential count was conducted using EDTA-stabilized whole blood (ADVIA 120 analyzer, Bayer Healthcare Diagnostics, Berlin, Germany).

Blood glucose was measured using a Radiometer ABL (Radiometer, Brønshøj, Denmark), or a fast-test system for diabetic patients.

Serum C-reactive protein (CRP) measurements were performed according to Heegaard et al. [23]. Briefly, CRP was analyzed using an ELISA and a pig serum pool calibrated against a human CRP calibrator (A0073, DAKO, Glostrup, Denmark) as the standard. Detection limit was 71 ng/mL (human equivalents) and all samples were run in duplicate.

Preparation of tracers

[99m]Tc-Nanocoll and ^{111}In-labeled leukocytes were prepared according to the instructions given by the producers. The ^{99m}Tc-Nanocoll kit was supplied by GE Healthcare, Brøndby, Denmark, and the ^{99m}Tc generator as well as the ^{111}In oxide was obtained from Mallinckrodt, Phamaceutical, København S, Denmark. The ^{111}In-labelling of leukocytes included isolation of the leukocyte fraction from autologous full blood using sedimentation and centrifugation [24]. Labeling efficacy of the leukocyte preparations were 82.5% for pig 1, 78.9% for pig 2, 70.0% for pig 3 and 62.0% for pig 4.

[11]C, [15]O and ^{18}F were produced at the PET Centre Aarhus using either a PETtrace 800 series cyclotron (GE Healthcare, Uppsala, Sweden) or a Cyclone 18/18 cyclotrone (IBA,

Table 1. Sequence of tracer injection for pig 1, bodyweight 40 kg, activity of tracers and time of diagnostic scan

Tracers and sequence	Time of injection	Activity	Time of diagnostic scan	Injection-scan interval
^{11}C-methionine	0 min	474 MBq	1 h 5 min	1 h 5 min
^{111}In-leukocytes	1 h 45 min	20,2 MBq	-A	-
^{11}C-PK11195	2 h 0 min	424 MBq	3 h 5 min	1 h 5 min
^{15}O-H$_2$O^B	4 h 23 min	500 MBq	Immediately	Immediately
^{99m}Tc-Nanocoll	6 h 30 min	500 MBq	7 h 15 min	45 min
^{111}In-leukocytes	-	-	7 h 15 min	5 h 30 min
^{68}Ga-citrate	10 h 35 min	173 MBq	12 h 35 min	2 h 0 min
^{18}F-FDG	14 h 16 min	299 MBq	15 h 50 min	1 h 34 min

^{A}-indicates that the information is irrelevant. ^{B}Results of ^{15}O-H$_2$O scan will be recorded elsewhere.

Louvain La Neuve, Belgium). ^{68}Ga was obtained by eluding a ^{68}Ge/^{68}Ga generator (IGG 100, Eckert & Ziegler AG Eurotope GmbH, Berlin, Germany).

^{18}F-FDG was produced by a standard procedure applying a GE Healthcare MX Tracerlab synthesizer, Mx cassettes supplied by Rotem Industries (Arava, Israel) and chemical kits supplied by ABX GmbH (Radeberg, Germany). The radiochemical purity was higher than 99%.

^{15}O-water was produced by burning of ^{15}O-oxygen with hydrogen gas on platinum catalyst at 250°C using a standard system supplied by GE Healthcare. The radiochemical purity exceeded 99%. The results of the ^{15}O-water scan will be reported elsewhere.

^{11}C-methionine was synthesized by [^{11}C] S-methylation of L-homocysteine thiolactone with methyl iodide [25] followed by preparative HPLC using a GE Healthcare Tracerlab FXC PRO, synthesizer. L-homocysteine thiolactone was supplied by Sigma (Sigma-Aldrich Denmark, Brøndby, Denmark). Other chemicals including iodine or acetone were supplied by either Aldrich (Sigma-Aldrich Denmark, Brøndby, Denmark) or Aarhus University Hospital Pharmacy (Aarhus, Denmark). The radiochemical purity exceeded 95% and the specific radioactivity generally was higher than 37 GBq/µmol.

^{11}C-PK11195 was prepared by N-methylation of desmethyl-PK11195 with methyl iodide [26] followed by preparative HPLC and solid phase extraction using a GE Healthcare Tracerlab FXC PRO, synthesizer. Desmethyl-PK11195 was supplied by ABX GmbH. Other chemicals were supplied by either Aldrich or Aarhus University Hospital Pharmacy. The radiochemical purity

exceeded 95% and the specific radioactivity generally was higher than 50 GBq/µmol.

^{68}Ga-citrate was synthesized in high yield within 10 min and without the use of organic solvents as described earlier [27]. The radiochemical purity exceeded 99%.

CT, SPECT and PET

At the day of the scan, i.e. 7 days after inoculation, the pig was essentially handled as described earlier [28]. Briefly, the pig was sedated with an im injection of 0.5 mg/kg bw midazolam prior to transport from the housing facility to PET Centre Aarhus. At the centre, the pig was injected im with 1.25 mg/kg bw midazolam and 6.25 mg/kg bw S-ketamine hydrochloride (S-ketamine, Pfizer Aps, Ballerup, Denmark) followed by anaesthesia with propofol and monitored as described above. Venous and arterial catheters were placed through a skin incision into the jugular vein and the common carotid artery, and the skin was sutured fixating the catheters. A catheter was placed in the urinary bladder to collect urine. After sampling of blood, labeling and reinjection of autologous leukocytes, and after ^{11}C-methionine, ^{11}C-PK11195 and ^{15}O-H$_2$O scans, the pig was disconnected from the respirator and the propofol pump, and transported to PET Centre Aalborg (approx. 1.5 h) attended by a veterinarian, where anaesthesia and monitoring was resumed, and the last scans performed. The pig was kept hydrated by the continuous infusion of up to 3 l of sterile 0.9% saline, and the body temperature was kept normal by the use of electrically heating blankets regulated by a rectal body-temperature measurement. The bw and sequence of tracer injections and scans for pig 1 is given in **Table 1**; the sequence for all

scanned pigs is presented in <u>Supplementary Table 1</u>.

All examinations at PET Centre Aarhus were performed with an integrated PET/CT system (Siemens Biograph True point 64 PET/CT, Siemens, Erlangen, Germany). The pigs were placed in dorsal recumbency (supine position), with the pelvic limbs in a slightly flexed position intended to secure that both the pelvic limbs and region could fit within one bed position (21 cm). Initially a topogram (scout view) was obtained to ensure body coverage from snout to tail. Attenuation correction of PET data was obtained first based on low dose CT maps. PET images were reconstructed with the iterative TrueX algorithm (Siemens, Erlangen, Germany). Co-registration for image fusion of CT and PET was done automatically by the system, based on calibration of the combined PET/CT scanner.

SPECT/CT (in Aalborg) was performed on the pelvic limbs and region included in a single bed position using a Symbia T16 SPECT/CT (Siemens Medical Solutions, Hoffman Estates, Illinois, USA). The residual activity from PET isotopes was recognized as a source of background radiation on the SPECT scanner, and optimal collimators to solve this problem were identified [29]. We applied the medium-energy collimators as suggested. At PET Centre Aalborg, PET/CTs were performed with an integrated system (GE VCT discovery True 64 PET/CT 2006, GE Healthcare, USA) essentially as in Aarhus, one bed position spanning 15 cm.

All PET scans were first performed as dynamic PET of the pelvic (hind) limbs and region followed by a later diagnostic (static) whole body scan of 5 min (PET Centre Aarhus) and 6 or 12 min (PET Centre Aalborg) duration per bed position. Planar images of whole body scintigraphies were also included in the protocol. Arterial blood samples were collected and tested for intact PET tracer content in order to determine input function and to allow kinetic modeling. However the results of the whole body scintigraphies, dynamic PET scans, ^{15}O-water scan and kinetic modeling will be reported elsewhere.

Reading the scans

Computed tomography with ^{18}F-FDG, ^{68}Ga-citrate, ^{11}C-PK11195, ^{11}C-Methionine, ^{99m}Tc-

Nanocoll and ^{111}In-leucocytes was read individually. PET and SPECT were also read as fused images with CT. All scans were evaluated by a nuclear physician and a veterinarian. Tracer accumulation in the right pelvic limb was regarded as pathological if morphological changes (CT) could be correlated to uptake or if increased accumulation was present compared to the same region of the non-inoculated left limb. The physiological (background) uptake and readability of the different tracers was also recorded.

Gross pathology and histopathology

Following euthanasia with a barbiturate (Pentobarbital natrium, Skanderborg Apotek, Skanderborg, Denmark), the carcass was kept at 4°C for approximately 8 h, transported for approximately 4 h at room temperature, and necropsied. Necropsy was performed according to Madsen and Jensen [30] and included mid-sagittal cutting (sawing) through the bones of both the right and left pelvic limbs (femur, femoral head and neck, patella, tibia, calcaneus, talus, tarsus, metatarsus III, metatarsus IV, and phalanges of toes III and IV) and the head. If indicated, for example by the presence of signs of spread of the infection, also mid-sagittal sectioning of the vertebral column, humerus, radius and ulna was performed. Necropsy also included inspection of the lymph nodes draining the pelvic limb, i.e. the right and left mammary, subiliac and medial iliac nodes.

Predefined tissues and organs were sampled for microbial cultivation. Biopsies were obtained from the lungs and the distal metaphyseal/physeal interface of both the right and left femur. Prior to sampling of bone biopsies, the following precautions were taken to avoid contamination: after freeing the femoral bone from soft tissues the distal half was submerged into 96% ethanol for 20 sec and a 2 mm drill was heated in boiling water for 10 sec; the drill was performed from the medial epicondyle towards the lateral one, spanning no less than 3/4 of the distance in between. Predefined tissues and organs were selected for histopathology including right and left medial iliac lymph nodes and bone from both the right and left pelvic limbs. Identification of gross lesions at necropsy generally resulted in additional sampling for microbiology and histopathology.

Table 2. Haematology of pigs before and after inoculation with *S. aureus* into the right femoral artery

Tests	Normal values[A]	Pig 1		Pig 2		Pig 3		Pig 4	
		-4pi[B]	+5pi[B]	0pi[B]	+7pi	-2pi	+7pi	-3pi	+7pi
Leukocytes, 10^9/L	11.3-22.8	19.9	22.5	19.2	30.4	21.6	15.2	NT[C]	21.9
Lymphocytes, 10^9/L	4.6-10.0	11.2	9.8	10.9	6.6	10.0	6.8	NT	4.2
Neutrophils, 10^9/L	3.1-9.6	3.3	9.5	5.8	20.3	9.7	7.4	NT	16.8
Eosinophils, 10^9/L	0.0-0.9	4.4	2.4	1.7	2.1	0.7	0.5	NT	0.4
Haemoglobin, mmol/L	6.2-9.4	6.9	7.0	6.7	5.2	6.8	7.5	NT	4.9
CRP, µg/mL	< 15.0	1.6	82.6	0.8	59.8	9.9	2.2	0.6	41.3
Glucose, mmol/L[D]	3.5-6.6	NT	NT	NT	3.8	NT	3.8	NT	3.1

[A]Normal values supplied by the Central Laboratory. For the C-reactive protein (CRP) the normal-value shown here (< 15 µg/mL) corresponds to the highest value recorded in 5 normal pigs presented in two different publications using the same CRP test as employed in the present study [20, 32]. [B]-4pi indicates blood sampling four days prior to inoculation, +5pi indicates sampling five days after inoculation, and 0pi indicates sampling immediately before inoculation. [C]NT indicates not tested. [D]Blood glucose was measured at the day of scan (+7pi) in pigs 2, 3 and 4.

ness of the right pelvic limb two to four days pi. Five to seven days pi, pigs 1, 2 and 4 displayed elevated numbers of blood neutrophils or neutrophilia and CRP levels also above normal values (**Table 2**). In pig 3 the neutrophil count had normalized and the CRP level had decreased seven days pi.

Significant lesions in the region studied, i.e. the pelvic limbs and pelvic region, were only present in the inoculated, right side, as presented in Supplementary Table 3. In pig 1 a subcutaneous cystic lesion developed at the inoculation site and histopathology showed a content of blood components, including erythrocytes and fibrin, in the centre and a wall composed of granulation tissue with occasional presence of exudated neutrophils. In pigs 1 and 4 *S. aureus* positive abscesses occurred in the soft tissues related to the inoculation site (**Figure 1A**). The lungs from pigs 1, 2 and 4 were positive for *S. aureus* indicating a generalized spread. The lungs from pig 3 were sterile as was the biopsy from the metaphyseal/physeal area of the right distal femur; this pig was not only without clinical signs, but also without any signs of infection by CT, PET, SPECT, gross pathology and haematology (**Table 2**). The bone biopsies from the left femurs (non-inoculated limbs) were sterile in pigs 2, 3 and 4, and the sparse growth (few colonies) of *Escherichia coli* in pig 1 was deemed to represent contamination.

In the three pigs that did develop infection, pig 1 had three osteomyelitis lesions, and pigs 2 and 4 had one focus each, as evidenced by CT scan, osteolysis and sequestration, combined with the gross pathology of suppurative osteomyelitis (**Figure 1B**). The osteomyelitis affecting the toes of pigs 1 and pig 4 were coherent with peripheral abscesses revealing *S. aureus* on culture (**Figure 1C**). The biopsy from the distal right femur was positive for *S. aureus* only in pig

For histopathology of soft tissues, samples were fixed in 3.7% neutral buffered formaldehyde for 4 days, kept in 70% ethanol for 3-5 weeks, dehydrated and embedded in paraffin wax, cut in 3 µm thick sections, mounted on glass slides, stained with haematoxylin and eosin or Masson trichrome, and cover slipped according to standard procedures [31].

Bone samples were fixed for 6-9 days in 3.7% neutral buffered formaldehyde and transferred to 3.3% formaldehyde with 17% formic acid for decalcification. This solution was replaced every week and after a total of 4-6 weeks, the bones had become soft and were processed for histology similar to soft tissues.

Results

Clinical assessment, CT, gross pathology, microbiology and histopathology

Three of the eight pigs inoculated with *S. aureus* were euthanized for ethical reasons before scans could be performed (Supplementary Table 2); the four scanned pigs were numbered sequentially 1 to 4. No clinical signs were present in pigs 1 to 4 prior to inoculation; pigs 1, 2 and 4 had normal values of blood neutrophils and serum CRP; pig 3 had neutrophilia (above normal values) and an elevated CRP level which was still within normal range. Two pigs (1 and 2) had eosinophilia before and after inoculation. The pigs, except pig 3, developed clinical signs of infection after inoculation. Pigs 1, 2 and 4 developed swelling and mild to moderate lame-
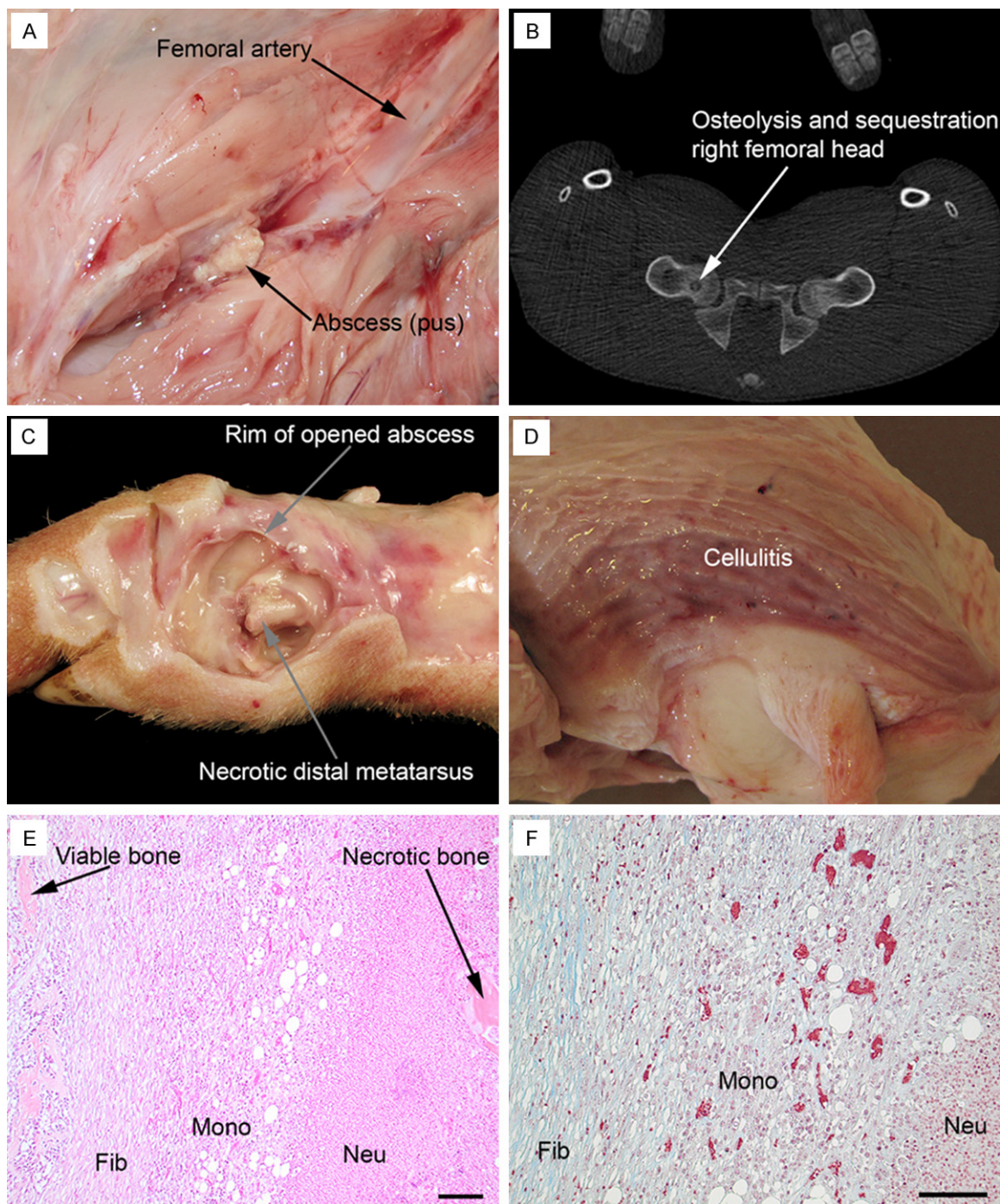
Figure 1. Gross pathology, CT and histopathology, pig 1, 2 and 4. (A) Small soft tissue abscess, approx. 1 cm in diameter, in the right pelvic limb, pig 1; compare to **Figure 3A**. (B) CT, transversal projection, of pelvis, pig 1; compare to **Figure 3A**. (C) Gross pathology of right metatarsus II, medial view, pig 4; the abscess peripheral to the bone has been opened and pus evacuated exposing necrotic metatarsus II bone and a pathological fracture along the growth plate in the distal part of the bone. (D) Cellulitis, i.e. grey-red edematous tissue, peripheral to right patella, pig 2; the cranial surface of patella is present in the lower right part of the picture. Haematoxylin and eosin (E) and Masson trichrome (F) staining (trichrome stains collagen blue) of the tissue bridging viable and necrotic bone components of the right distal metatarsus III, pig 1; fibroblasts (Fib) with collagen formation, mononuclear cells (Mono) and neutrophilic granulocytes (Neu); bar = 100 μm.

1. This corresponded to the finding of an osteomyelitis lesion in this location in pig 1, and

absence of lesions with this location by CT and gross pathology in pigs 2 and 4. Histopathology

Figure 2. Whole body ^{68}Ga-citrate PET, maximum intensity projection (MIP), pig 1. Physiological accumulation in the growth zones (metaphyses) of the bones.

was performed on the osteomyelitis lesions in the distal femur and distal metatarsus III of pig 1, and distal metatarsus II of pig 4. The lesions were necrotizing and suppurative, and surrounded by an inflammatory tissue without bone structures (osteolysis), but composed of undifferentiated mononuclear cells, some fibroblasts and light amounts of collagen (**Figure 1E** and **1F**). By these criteria the osteomyelitis lesions were subacute. Lesions were present in

both the metaphyseal and epiphyseal areas, communicating through inflammatory/infectious defects in the cartilaginous growth disc in the long bones. The histopathology of the osteomyelitis in patella was similar to that of the long bones, but disclosed an acute stage with lack of e.g. undifferentiated mononuclear cells and fibroblasts. The osteomyelitis of the patella communicated with the synovial space of the *S. aureus* infected knee joint and with the peripheral soft tissue lesions by inflammatory/infectious fissures in the peripheral articular cartilage and fibrocartilaginous tissue, respectively.

Two additional bone lesions were identified in the right tibia of pig 1. The proximal and distal physis region of tibia disclosed osteolysis by CT, no lesions by gross pathology (only one midsagittal cut performed), and histopathology and microbiology was not performed.

The soft tissue (cutis and subcutis) peripheral to the right, osteomyelitis-affected, patella in pig 2 was *S. aureus* positive by cultivation and had small, barely visible, abscesses and also a diffuse inflammatory reaction (**Figure 1D**). Histopathology revealed an edematous tissue with areas of haemorrhage and fibrin exudation, a light diffuse exudation of neutrophils and macrophages, fibroblast proliferation, and extensive accumulation of fibrin and neutrophils in dilated lymph vessels, i.e. cellulitis.

By gross pathology the right medial iliac lymph nodes of pigs 1, 2 and 4 were all enlarged. Histopathology disclosed edema and a light exudative response (fibrin, neutrophils and macrophages) in connective tissue trabeculae, protein containing dilated lymph vessels, and erythro-phagocytosis located to the medulla. In pig 2, the trabeculae also showed a light fibroblastic response and areas with extracellular or intracellular located eosinophilic material were identified in the nonfollicular part of the cortex. The material occasionally contained nuclear remnants, and thus could represent presence of tingible-body macrophages. These cells could sometimes be associated with peripherally located neutrophils, which also infiltrated other parts of the cortex and medulla. All lymph nodes had a light medullar and cortical eosinophilic infiltrate, which could also be found in the contralateral left nodes. One of the left nodes (pig 2) had an acute micro-abscess, but none of

Table 3. Number of gross pathology and/or CT lesions identified by the individual tracers

Lesion	Total number	Tracers				
		^{18}F-FDG	^{68}Ga-citrate	^{11}C-methionine	^{11}C-PK11195	^{111}In-leukocytes
Osteomyelitis	5	4	1	2	0	4[A]
Soft tissue abscess	5	5	3	4	1	4
Arthritis	3	0	0	0	0	0
Enlarged lymph node	5	3	2	2	1	0[B]

[A]In one of these four lesions, the patella, the ^{111}In-leukocytes had only accumulated in the cortical part of the bone. [B]Only two lymph nodes were scanned.
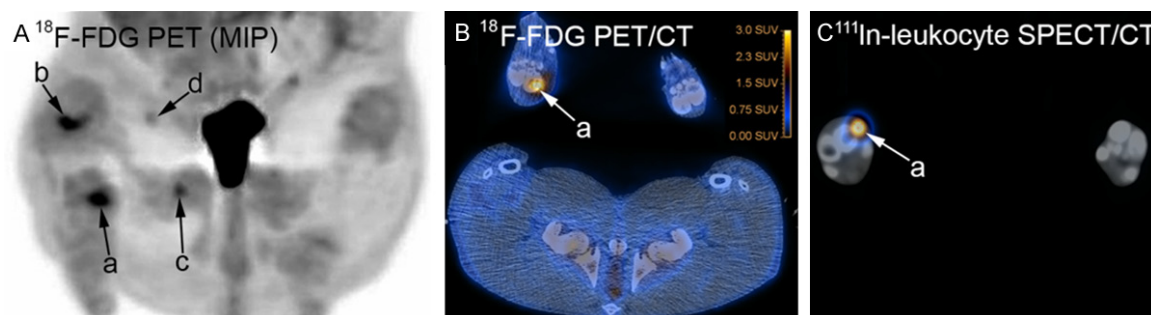

Figure 3. Scans of pelvic (hind) limbs and region, pig 1. A: Tracer accumulation is evident in the right hind limb in the distal metatarsus III (a), distal femur (b), femoral head and neck (c), and the small abscess in the cranio-medial thigh muscle region (d); compare accumulation "c" to **Figure 1B** and "d" to **Figure 1A**; the urinary bladder (in the center) has prominent ^{18}F-FDG accumulation. B: Transversal projection; accumulation of tracer in osteolytic metatarsus III of the right hind limb (a). C: Transversal projection; accumulation of tracer in abscess peripheral to the osteolytic metatarsus III of the right hind limb (a).

the medial iliac lymph nodes were sampled for microbiology. The mammary lymph nodes in pigs 1 and 4 were enlarged also as judged by CT, but histopathology and microbiology were not performed.

Physiological (background) tracer uptake

Looking at the pelvic limbs and region only, ^{11}C-methionine and ^{11}C-PK11195 accumulated in both soft tissue and bone in a coarse, speckled pattern. Accumulation increased from barely visible in the soft tissues to being more pronounced in bones excluding the diaphyses. The ^{68}Ga-citrate tracer expressed an intense, homogenous accumulation in the growth zones (metaphyses) of the bones with other parts of bones and soft tissue displaying a light and homogenous accumulation (**Figure 2**). ^{18}F-FDG accumulated only lightly and homogenously in bones occasionally accentuating growth zones. ^{111}In-leukocytes and ^{99m}Tc-Nanocoll displayed a homogenous and fairly intense accumulation in the bones only, although the diaphyses showed only moderate activity.

Performance of the tracers

Supplementary Table 3 aligns the CT-, PET-, SPECT-, gross pathology and microbiological findings. Significant lesions in the pelvic limbs and region were only present in the right side. The osteolytic lesions in the proximal and distal physis region in the tibia in pig 1 accumulated ^{18}F-FDG and ^{111}In-leukocytes, respectively. We did not find any lesions here by gross pathology, but only one mid-sagittal cut was performed (and the lesions may have been missed), and microbiology and histopathology was not performed. The subcutaneous cystic lesion at the inoculation site in pig 1 did not accumulate any of the tracers. The cause of the ^{111}In leukocyte accumulating lesion deep in the caudal thigh muscles of pig 2 was uncertain. Disregarding these four lesions and the two characterized by edema only, the study comprises 13 infectious lesions (five osteomyelitis lesions, five abscesses/cellulitis and three joints with arthritis) and five enlarged lymph nodes. **Table 3** summarizes the performance of the tracers on these 18 lesions. None of the tracers tested accumulat-

A ^{18}F-FDG PET

B ^{68}Ga-citrate PET

C ^{11}C-methionine PET

D ^{11}C-PK11195 PET

E ^{111}In-leukocyte SPECT

nine (panel C) and ^{11}C-PK11195 (panel D) identifies the mammary lymph node, and focal accumulation (c) of ^{111}In-leukocytes (panel E) identify the abscess; with ^{68}Ga-citrate, the mammary lymph node is barely visible (d).

ed in joints with arthritis. By comparing the remaining 10 infectious lesions, ^{18}F-FDG accumulated in nine and ^{111}In-leukocytes accumulated in eight of the lesions (**Figure 3A-C**); ^{11}C-methionine accumulated in six, ^{68}Ga-citrate accumulated in four and ^{11}C-PK11195 accumulated in only one of the lesions. ^{18}F-FDG only failed to accumulate in the osteomyelitis affected patella of pig 2, and here ^{111}In-leukocytes accumulated in the cortical part only; the scan with ^{99m}Tc-Nanocoll revealed a complete lack of medullary activity, which was in contrast to the contralateral patella and the bones of the pigs in general. In pig 1 ^{111}In-leukocytes (labeling efficacy was 82.5%) did not accumulate in one of the osteomyelitis lesion (femoral head and neck), and in one small abscess with a diameter of approx. 1 cm, both lesions being positive by ^{18}F-FDG (**Figures 1A and 3A**). ^{11}C-PK11195 accumulated in the tissue peripheral to patella of pig 2 only, a location which was marked by all other PET tracers and ^{111}In-leukocytes as well. The large subcutaneous located abscess in pig 4 accumulated all PET tracers, except ^{11}C-PK11195, and also ^{111}In-leukocytes (**Figure 4A-E**).

Four of the five enlarged lymph nodes accumulated PET tracers. The two lymph nodes that were SPECT scanned did not
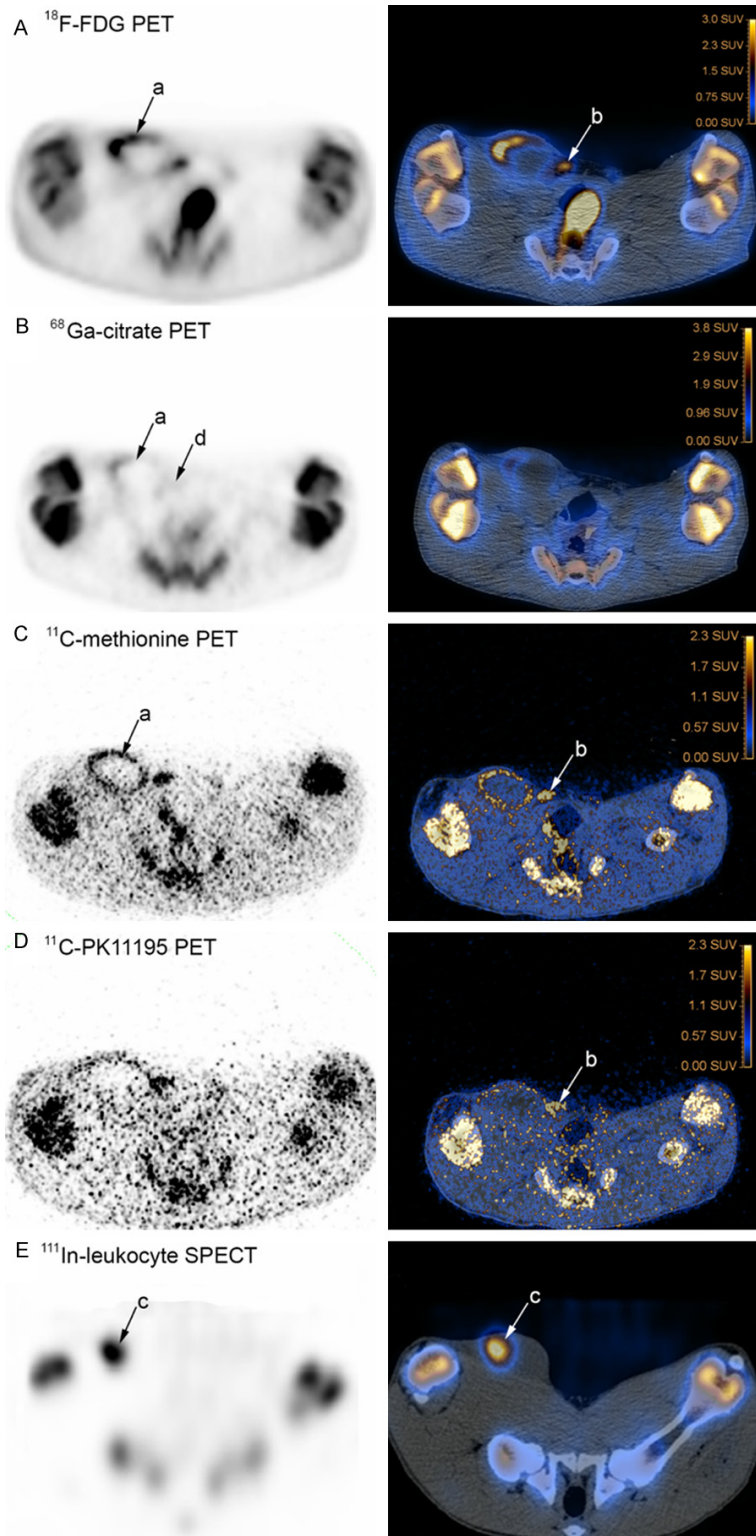
Figure 4. Scans of pelvic (hind) limbs and region, PET and SPECT to the left, and CT fused images to the right, transversal projections, pig 4. Tracers have accumulated in lesions in the right side of the pig. Sphere-formed accumulations (a) with ^{18}F-FDG (panel A), ^{68}Ga-citrate (panel B) and ^{11}C-methionine (panel C) outline the large, approx. 8 cm in diameter, subcutaneous located abscess; focal accumulation (b) with ^{18}F-FDG (panel A), ^{11}C methio-

accumulate leukocytes, but both of these did accumulate PET tracers. **Figure 4A-D** show a comparison of PET tracer accumulation in the mammary lymph node from pig 4.

Discussion

In this study four pigs with a total of 13 infectious lesions and 5 enlarged lymph nodes were scanned. ^{111}In-leukocyte SPECT and ^{18}F-FDG PET were superior in visualizing the infectious lesions. The leukocyte scans were performed on average 6 h after injection of the labeled leukocytes, as opposed to the traditional 24 to 48 h of post-injection time-lapse in humans [33], but these early images performed well. However, the SPECT scan missed two lesions which accumulated ^{18}F-FDG, and disregarding the cortical accumulation of labeled leukocytes in patella of pig 2, both tracers failed to mark the lesion there. Both ^{11}C-methionine and ^{68}Ga-citrate were able to accumulate in infectious bone and soft tissue lesions, but to a lesser extent compared to labeled leukocytes and ^{18}F-FDG. The ^{11}C-methionine and ^{68}Ga-citrate tracers should, however, be explored more thoroughly for use in soft tissue infection, as ^{68}Ga-citrate accumulated in three and ^{11}C-methionine accumulated in four of the five soft tissue lesions.

The patellar lesion which did not accumulate either ^{18}F-FDG or labeled leukocytes also showed lack of bone marrow activity by ^{99m}Tc-Nanocoll. Usually inflammatory and infectious lesions in the bone marrow will accumulate ^{18}F-FDG and labeled leukocytes, but not ^{99m}Tc-Nanocoll [34]. An explanation for the unusual combination of scans could be the occurrence of patellar ischaemia shortly after inoculation which would make it impossible for the tracers to reach the medulla later at scanning, and also would prevent healing at least in the central part of the lesion. Indeed, histopathology of the patella disclosed an acute necrotizing and suppurative bone infection, indicating both ischaemia and lack of reparatory processes, i.e. lack of progression to a subacute stage. It is well known that the pathogenesis of hematogenous osteomyelitis in juvenile individuals (man and animals) includes, at least in the long bones, thrombosis and increased intraosseous pressure within the medulla [7, 35].

Juvenile haematogenous osteomyelitis has an incidence of 1.94-13/100,000 in high-income countries [36, 37] but it is much more common in low-income countries. Musculoskeletal impairment due to infection has been estimated to affect 12 million (3%) of children in the least developed countries of the world with chronic haematogenous osteomyelitis being a major cause [38]. Prompt diagnosis and therapy is of particular importance in cases of aggressive and multifocal disease, which was modeled in the present porcine study and also reported previously [9], to prevent the local spread through growth plates, into joints and laterally through cortex and periosteum to form contiguous soft tissue abscesses and cortical sequesters and involucra. Bone scan and CT is part of the diagnostic algorithm in children suspected of acute osteomyelitis [8]. The increasing radiation exposure and concern about long tracer half lives of CT, bone-SPECT/CT (not performed here), PET/CT and leukocyte-SPECT/CT should be balanced against the likely faster diagnostics, which can prevent a protracted course and disabling disease. We did not at first identify the osteolytic lesion in the femoral head and neck in pig 1, but the ^{18}F-FDG accumulation drew our attention to the lesion. The osteolytic nature of the two foci in the proximal and distal tibia of pig 1, respectively, was also first recognized from the PET (^{18}F-FDG) or leukocyte SPECT, but the two lesions were not validated further by pathology and microbiology.

The ^{11}C-methionine scans displayed a speckled appearance, indicating low activity of the radiotracer, which corresponds to the 20 min half-life of the ^{11}C-nuclide and scans being read 1 h and 5 min after injection. Thus, dynamic scans could add to a more thorough evaluation on the performance of ^{11}C-methionine by indicating the optimal scan time point. The selective accumulation in lesions also needs to be scrutinized, as the increased vascular permeability and increased blood flow characteristic of inflammation by itself may cause local tracer uptake. ^{11}C-methionine accumulated physiologically in the bones, excluding the diaphyses, as did in particular the ^{68}Ga-citrate tracer in the growth zones, and this could prevent the use of these tracers to support the identification of haematogenous osteomyelitis in juvenile individuals; accumulation of ^{68}Ga-citrate (i.e. the ^{68}Ga ions) in the growth plate of bone has been reported previously in rats, but the age of the rats was not specified [19]. One experimental study in mature rats demonstrated that

[68]Ga-citrate accumulated in *S. aureus* infected bone but not in healing bone, which was in contrast to ^{18}F-FDG, that accumulated in both types of lesions [39]. In a study comprising 31 patients with bone infections, mean age 42 years, it was concluded that ^{68}Ga-citrate may have a possible role in diagnosing bone infections, and that ^{68}Ga-citrate seems to be a specific marker of bone prostheses infection [18].

[68]Ga-citrate accumulated in three and ^{11}C-methionine accumulated in four of the five soft tissue lesions, and their use in soft tissue infection should be explored. In a study in rats, experimentally induced *S. aureus* soft tissue abscesses accumulated ^{68}Ga-citrate 3-4 days after inoculation [19]. Methionine labeled with carbon nuclides has previously been demonstrated to differentiate between suppurative and granulomatous inflammation (low uptake) and tumors (high uptake) in a rat study [11]. The obvious sphere-formed accumulation of ^{11}C-methionine in the abscess of pig 4 (**Figure 4C**) indicates selective labeling of the abscess capsule, which contrasts the inclusion of some luminal labeling by ^{18}F-FDG and the selective luminal labeling by ^{111}In-leukocytes (**Figure 4E**).

All of the tested PET tracers possessed the ability to accumulate in the lymph nodes. Histopathology of the regional lymph nodes of the infected right hind limb (only medial iliac lymph nodes examined) were indicative of increased drainage and edema. However, only the lymph node from pig 2 had changes which could indicate a lymphocytic hyperplastic response evidenced by the presence of tingible body macrophages. This type of cells contain phagocytosed apoptotic (tingible) bodies formed during lymphocytic proliferation and differentiation [40]. Adding a stereological approach to our protocol would make it possible to quantify the number of proliferating cells of a particular lymph node, and thus to prove the ability of the tracers to accumulate in response to either inflammation/infection or proliferation or both. Draining lymph nodes accumulated ^{18}F-FDG, ^{11}C-methionine and ^{67}Ga-citrate in *Escherichia coli* infection in rats, but a differentiation between lymphadenitis and hyperplasia was not performed [41].

We proved it possible to use a sequential tracer injection- and scan protocol, having the pigs anaesthetized for a total of approximately 18 h. However, the experimental setup originally included eight pigs that were inoculated with *S. aureus* into the femoral artery as described by Johansen et al. [9, 10]. Three of the pigs had to be euthanized for ethical reasons before scans could be performed. The main limitation of this study is the small number of pigs, presenting a total of 13 infectious lesions and 5 enlarged lymph nodes, and thus the descriptive nature of the study. In the three infected pigs out of the four scanned, clear signs of systemic spread were recognized by the positive lung culture, the lung being a primarily blood-filtering organ in several animal species including pigs [42]. In the original paper by Johansen et al. [9], spread from the chronic lesions in the bones to induce acute lung and bone lesions were observed in one out of three animals. Thus we experienced difficulties in reproducing the model completely as described [9], and future studies using the model should include means to prevent generalized spread of the infection. The successful prevention of spread will reduce suffering and limit the number of animals used, and also prevent accidental seeding of bacteria to the non-inoculated limb which may influence the interpretation of the scan results. Some optimization of gross pathology, microbiology and histopathology methods to disclose and characterize the lesions induced is also warranted. For example, more attention should be put on a thorough characterization of all regional lymph nodes, and bone lesions not recognized by gross pathology might be so by applying a stereological sampling protocol for histopathology, which at the same time could allowed for estimation of the size of the lesion (volume and surface area).

In conclusion, we were able to scan *S. aureus* infected pigs using a sequential 18 h long scan protocol and seven different tracers. ^{18}F-FDG PET was superior to ^{111}In-leukocyte SPECT, performed as early scans 6 h after injection of the leukocytes, to find infectious and proliferative, i.e. hyperplastic, lesions. ^{11}C-PK11195 only accumulated in one out of ten of the infectious lesions. ^{11}C-methionine and possibly ^{68}Ga-citrate may be useful for diagnosis of soft tissue lesions, but were only able to visualize two respectively one of the five osteomyelitis lesions.

Acknowledgements

Disclosure of conflict of interest

None.

Address correspondence to: Dr. Ole L Nielsen, Department of Veterinary Disease Biology, University of Copenhagen, Ridebanevej 3, DK-1870 Frederiksberg C, Denmark. E-mail: oleni@sund.ku.dk

References

[1] Carek PJ, Dickerson LM and Sack JL. Diagnosis and management of osteomyelitis. Am Fam Physician 2001; 63: 2413-2420.

[2] Berbari EF, Steckelberg JM and Osmon DR. Osteomyelitis. In: Mandell GL, Bennett JE and Dolin R, editors. Mandell, Douglas, and Bennett's Principles and Practice of Infectious Diseases. Volume 1. 6th edition. Livingstone: Elsevier Churchill; 2005. pp. 1322-1332.

[3] Lew DP and Waldvogel FA. Osteomyelitis. Lancet 2004; 364: 369-379.

[4] van der Bruggen W, Bleeker-Rovers CP, Boerman OC, Gotthardt M and Oyen WJ. PET and SPECT in osteomyelitis and prosthetic bone and joint infections: a systematic review. Semin Nucl Med 2010; 40: 3-15.

[5] Termaat MF, Raijmakers PG, Scholten HJ, Bakker FC, Patka P and Haarman HJ. The accuracy of diagnostic imaging for the assessment of chronic osteomyelitis: a systematic review and meta-analysis. J Bone Joint Surg Am 2005; 87: 2464-2471.

[6] Connolly LP, Connolly SA, Drubach LA, Jaramillo D and Treves ST. Acute hematogenous osteomyelitis of children: assessment of skeletal scintigraphy-based diagnosis in the era of MRI. J Nucl Med 2002; 43: 1310-1316.

[7] Steer AC and Carapetis JR. Acute hematogenous osteomyelitis in children: recognition and management. Paediatr Drugs 2004; 6: 333-346.

[8] Peltola H and Paakkonen M. Acute osteomyelitis in children. N Engl J Med 2014; 370: 352-360.

[9] Johansen LK, Koch J, Frees D, Aalbaek B, Nielsen OL, Leifsson PS, Iburg TM, Svalastoga E, Buelund LE, Bjarnsholt T, Hoiby N and Jensen HE. Pathology and biofilm formation in a porcine model of staphylococcal osteomyelitis. J Comp Pathol 2012; 147: 343-353.

[10] Johansen LK, Svalastoga EL, Frees D, Aalbaek B, Koch J, Iburg TM, Nielsen OL, Leifsson PS and Jensen HE. A new technique for modeling of hematogenous osteomyelitis in pigs: inoculation into femoral artery. J Invest Surg 2013; 26: 149-153.

[11] Zhao S, Kuge Y, Kohanawa M, Takahashi T, Zhao Y, Yi M, Kanegae K, Seki K and Tamaki N. Usefulness of 11C-methionine for differentiating tumors from granulomas in experimental rat models: a comparison with 18F-FDG and 18F-FLT. J Nucl Med 2008; 49: 135-141.

[12] Harris SM, Davis JC, Snyder SE, Butch ER, Vavere AL, Kocak M and Shulkin BL. Evaluation of the biodistribution of 11C-methionine in children and young adults. J Nucl Med 2013; 54: 1902-1908.

[13] Cagnin A, Gerhard A and Banati RB. In vivo imaging of neuroinflammation. Eur Neuropsychopharm 2002; 12: 581-586.

[14] Pugliese F, Gaemperli O, Kinderlerer AR, Lamare F, Shalhoub J, Davies AH, Rimoldi OE, Mason JC and Camici PG. Imaging of vascular inflammation with [11C]-PK11195 and positron emission tomography/computed tomography angiography. J Am Coll Cardiol 2010; 56: 653-661.

[15] Ren W, Muzik O, Jackson N, Khoury B, Shi T, Flynn JC, Chakraborty P and Markel DC. Differentiation of septic and aseptic loosening by PET with both 11C-PK11195 and 18F-FDG in rat models. Nucl Med Commun 2012; 33: 747-756.

[16] Hoffer P. Gallium: mechanisms. J Nucl Med 1980; 21: 282-285.

[17] Palestro CJ, Brown ML, Greenspan BS, McAfee JG, Royal HD, Schauwecker DS, Seabold JE and Signore A. Society of Nuclear Medicine Procedure Guideline for Gallium Scintigraphy in Inflammation Version 3.0, approved June 2, 2004. Rome: University La Sapienza; 2004. pp. 1-5.

[18] Nanni C, Errani C, Boriani L, Fantini L, Ambrosini V, Boschi S, Rubello D, Pettinato C, Mercuri M, Gasbarrini A and Fanti S. 68Ga-citrate PET/CT for evaluating patients with infections of the bone: preliminary results. J Nucl Med 2010; 51: 1932-1936.

[19] Kumar V, Boddeti DK, Evans SG and Angelides S. (68)Ga-Citrate-PET for diagnostic imaging of infection in rats and for intra-abdominal infection in a patient. Curr Radiopharm 2012; 5: 71-75.

[20] Leifsson PS, Iburg T, Jensen HE, Agerholm JS, Kjelgaard-Hansen M, Wiinberg B, Heegaard PM, Astrup LB, Olsson AE, Skov MG, Aalbaek B and Nielsen OL. Intravenous inoculation of Staphylococcus aureus in pigs induces severe sepsis as indicated by increased hypercoagu-

lability and hepatic dysfunction. FEMS Micro-biol Lett 2010; 309: 208-216.

[21] Hasman H, Moodley A, Guardabassi L, Stegger M, Skov RL and Aarestrup FM. spa type distribution in Staphylococcus aureus originating from pigs, cattle and poultry. Vet Microbiol 2010; 141: 326-331.

[22] Nielsen OL, Iburg T, Aalbaek B, Leifsson PS, Agerholm JS, Heegaard P, Boye M, Simon S, Jensen KB, Christensen S, Melsen K, Bak AK, Backman ER, Jorgensen MH, Groegler DK, Jensen AL, Kjelgaard-Hansen M and Jensen HE. A pig model of acute Staphylococcus aureus induced pyemia. Acta Vet Scand 2009; 51: 14.

[23] Heegaard PM, Pedersen HG, Jensen AL and Boas U. A robust quantitative solid phase immunoassay for the acute phase protein C-reactive protein (CRP) based on cytidine 5'-diphosphocholine coupled dendrimers. J Immunol Methods 2009; 343: 112-118.

[24] Roca M, de Vries EF, Jamar F, Israel O and Signore A. Guidelines for the labelling of leucocytes with (111)In-oxine. Inflammation/Infection Taskgroup of the European Association of Nuclear Medicine. Eur J Nucl Med Mol Imaging 2010; 37: 835-841.

[25] Comar D, Cartron J, Maziere M and Marazano C. Labelling and metabolism of methionine-methyl-11 C. Eur J Nucl Med 1976; 1: 11-14.

[26] Shah F, Hume SP, Pike VW, Ashworth S and Mc-Dermott J. Synthesis of the enantiomers of [N-methyl-11C]PK 11195 and comparison of their behaviours as radioligands for PK binding sites in rats. Nucl Med Biol 1994; 21: 573-581.

[27] Jensen SB, Nielsen KM, Mewis D and Kaufmann J. Fast and simple one-step preparation of (6)(8)Ga citrate for routine clinical PET. Nucl Med Commun 2013; 34: 806-812.

[28] Alstrup AKO and Winterdahl M. Imaging Techniques in Large Animals. Scand J Lab Animal Sci 2009; 36: 55-66.

[29] Jodal L, Afzelius P and Jensen SB. Influence of positron emitters on standard gamma-camera imaging. J Nucl Med Technol 2014; 42: 42-50.

[30] Madsen LW and Jensen HE. In: Jensen HE, editor. Necropsy of the Pig. Necropsy A Handbook and Atlas. Frederiksberg: Biofolia; 2011. pp. 83-106.

[31] Gamble M, Jones ML, Bancroft JD and Gamble M. The Hematoxylins and Eosin. Connective Tissue and Stains. In: Bancroft JD and Gamble M, editor. Theory and Practice of Histological Techniques. 6th edition. Churchill Livingstone Elsevier 2008; pp. 121-134, 135-160.

[32] Soerensen KE, Nielsen OL, Jensen HE, Leifsson PS and Iburg TM. Pulmonary Lesions Following Intravenous Inoculation with A High Concentration of Staphylococcus Aureus in Pigs. J Comp Pathol 2010; 143: 324-324.

[33] Palestro CJ, Brown ML, Forstrom LA, McAfee JG, Royal HD, Schauwecker DS, Seabold JE and Signore A. Society of Nuclear Medicine Procedure Guideline for 111In-Leukocyte Scintigraphy for Suspected Infection/Inflammation Version 3.0, approved June 2, 2004. Rome: University La Sapienza 2004; pp. 1-6.

[34] Palestro CJ, Love C, Tronco GG, Tomas MB and Rini JN. Combined labeled leukocyte and technetium 99m sulfur colloid bone marrow imaging for diagnosing musculoskeletal infection. Radiographics 2006; 26: 859-870.

[35] Emslie KR, Fenner LM and Nade SML. Acute Hematogenous Osteomyelitis .2. the Effect of A Metaphyseal Abscess on the Surrounding Blood-Supply. J Pathol 1984; 142: 129-134.

[36] Gafur OA, Copley LA, Hollmig ST, Browne RH, Thornton LA and Crawford SE. The impact of the current epidemiology of pediatric musculoskeletal infection on evaluation and treatment guidelines. J Pediatr Orthop 2008; 28: 777-785.

[37] Riise OR, Kirkhus E, Handeland KS, Flato B, Reiseter T, Cvancarova M, Nakstad B and Wathne KO. Childhood osteomyelitis-incidence and differentiation from other acute onset musculoskeletal features in a population-based study. BMC Pediatr 2008; 8: 45.

[38] Jones HW, Beckles VL, Akinola B, Stevenson AJ and Harrison WJ. Chronic haematogenous osteomyelitis in children: an unsolved problem. J Bone Joint Surg Br 2011; 93: 1005-1010.

[39] Makinen TJ, Lankinen P, Poyhonen T, Jalava J, Aro HT and Roivainen A. Comparison of 18F-FDG and 68Ga PET imaging in the assessment of experimental osteomyelitis due to Staphylococcus aureus. Eur J Nucl Med Mol Imaging 2005; 32: 1259-1268.

[40] Willard-Mack CL. Normal structure, function, and histology of lymph nodes. Toxicol Pathol 2006; 34: 409-424.

[41] Sugawara Y, Gutowski TD, Fisher SJ, Brown RS and Wahl RL. Uptake of positron emission tomography tracers in experimental bacterial infections: a comparative biodistribution study of radiolabeled FDG, thymidine, L-methionine, 67Ga-citrate, and 125I-HSA. Eur J Nucl Med 1999; 26: 333-341.

[42] Brain JD, Molina RM, DeCamp MM and Warner AE. Pulmonary intravascular macrophages: their contribution to the mononuclear phagocyte system in 13 species. Am J Physiol 1999; 276: 146-154.

Supplementary Table 1. Body weight of pigs at scan, sequence of tracer injection, activity of tracers and time of diagnostic scan

Scan sequence								
Pig 1, body weight 40 Kg	^{11}C-methionine	^{111}In-leukocytes	^{11}C-PK11195	^{15}O-H$_2$O^A	^{99m}Tc-Nanocoll	^{111}In-leukocytes	^{68}Ga-citrate	^{18}F-FDG
Time of injection	0 min	1 h 45 min	2 h 0 min	4 h 23 min	6 h 30 min	-	10 h 35 min	14 h 16 min
Activity	474 MBq	20.2 MBq	424 MBq	500 MBq	500 MBq	-	173 MBq	299 MBq
Time of scan	1 h 5 min	-	3 h 5 min	Immediately	7 h 15 min	7 h 15 min	12 h 35 min	15 h 50 min
Inj.-scan interval	1 h 5 min	-	1 h 5 min	Immediately	45 min	5 h 30 min	2 h 0 min	1 h 34 min
Pig 2, body weight 40 Kg	^{11}C-methionine	^{111}In-leukocytes	^{11}C-PK11195	^{15}O-H$_2$O^A	^{99m}Tc-Nanocoll	^{111}In-leukocytes	^{68}Ga-citrate	^{18}F-FDG
Time of injection	0 min	1 h 25 min	2 h 5 min	4 h 8 min	6 h 34 min	-^{B}	9 h 16 min	13 h 27 min
Activity	408 MBq	21.0 MBq	414 MBq	1000 MBq	500 MBq	-	113 MBq	389 MBq
Time of scan	1 h 5 min	-	3 h 10 min	Immediately	7 h 39 min	7 h 39 min	11 h 29 min	14 h 34 min
Inj.-scan interval	1 h 5 min	-	1 h 5 min	Immediately	1 h 5 min	6 h 14 min	2 h 13 min	1 h 7 min
Pig 3, body weight 39 Kg	^{11}C-methionine	^{111}In-leukocytes	^{15}O-H$_2$O^A	^{11}C-PK11195	^{99m}Tc-Nanocoll	^{111}In-leukocytes	^{68}Ga-citrate	^{18}F-FDG
Time of injection	0 min	1 h 24 min	1 h 54 min^C	2 h 37 min	6 h 21 min	-	9 h 6 min	13 h 24 min
Activity	500 MBq	14.3 MBq	1000 MBq	464 MBq	500 MBq	-	150 MBq	365 MBq
Time of scan	1 h 5 min	-	Immediately	3 h 42 min	7 h 1 min	7 h 1 min	11 h 9 min	14 h 24 min
Inj.-scan interval	1 h 5 min	-	Immediately	1 h 5 min	40 min	5 h 37 min	2 h 3 min	1 h 0 min
Pig 4, body weight 42 Kg	^{15}O-H$_2$O^A	^{11}C-methionine	^{111}In-leukocytes	^{11}C-PK11195	^{99m}Tc-Nanocoll	^{111}In-leukocytes	^{68}Ga-citrate	^{18}F-FDG
Time of injection	0 min	45 min	1 h 24 min	3 h 03 min	6 h 59 min	-	9 h 22 min	13 h 52 min
Activity	850 MBq	498 MBq	17.8 MBq	263 MBq	500 MBq	-	175 MBq	389 MBq
Time of scan	Immediately	1 h 50 min	-	4 h 8 min	7 h 52 min	7 h 52 min	11 h 22 min	14 h 59 min
Inj.-scan interval	Immediately	1 h 5 min	-	1 h 5 min	53 min	6 h 28 min	2 h 0 min	1 h 7 min

^{A}Results of ^{15}O-H$_2$O scan will be recorded elsewhere. ^{B}-indicates that the information is irrelevant. ^{C}A second ^{15}O-H$_2$O scan was performed: injection at 2 h 15 min with 1000 MBq.

Supplementary Table 2. Haematology of pigs before and after inoculation with S. *aureus* into the right femoral artery

Normal Tests values[A]		Pig 1		Pig 2		Pig 3		Pig 4		Pig 1-X[B]		Pig 2-X[B]		Pig 3-X[B]		Pig 4-X[B]	
		-4pi[C]	+5pi[C]	0pi[C]	+7pi	-2pi	+7pi	-3pi	+7pi	-4pi	+5pi	0pi	+4pi	-2pi	+4pi	-3pi	+4pi
Leukocytes (10^9/L)	11.3-22.8	19.9	22.5	19.2	30.4	21.6	15.2	NT[D]	21.9	16.5	25.6	17.9	18.1	22.3	NT	13.7	13.0
Lymphocytes (10^9/L)	4.6-10.0	11.2	9.8	10.9	6.6	10.0	6.8	NT	4.2	9.5	6.6	9.8	7.3	12.5	NT	7.0	7.7
Neutrophils (10^9/L)	3.1-9.6	3.3	9.5	5.8	20.3	9.7	7.4	NT	16.8	5.1	16.9	6.7	8.7	8.5	NT	5.4	4.0
Eosinophils (10^9/L)	0.0-0.9	4.4	2.4	1.7	2.1	0.7	0.5	NT	0.4	0.7	1.1	1.0	0.9	0.6	NT	0.8	0.7
Haemoglobin (mmol/L)	6.2-9.4	6.9	7.0	6.7	5.2	6.8	7.5	NT	4.9	7.4	7.3	6.7	5.5	6.8	NT	6.6	6.1
CRP (µg/mL)	< 15.0	1.6	82.6	0.8	59.8	9.9	2.2	0.6	41.3	2.0	62.3	2.0	NT	1.5	44.3	1.0	34.6
Glucose (mmol/L)[E]	3.5-6.6	NT	NT	NT	3.8	NT	3.8	NT	3.1	NT	NT	NT	NT	NT	NT	NT	NT

[A]Normal values supplied by the Central Laboratory. For the C-reactive protein (CRP) the normal-value shown here (< 15 µg/mL) corresponds to the highest value recorded in 5 normal pigs presented in two different publications using the same CRP test as employed in the present study [1, 2]. [B]Pig 1-X was not scanned because scanners and laboratory facilities were unavailable, and pig, 2-X, 3-X and 4-X were euthanized prior to scanning for ethical reasons (humane endpoints reached). [C]-4pi indicates blood sampling four days prior to inoculation, +5pi indicates sampling five days after inoculation, and 0pi indicates sampling immediately before inoculation. [D]NT indicates not tested. [E]Blood glucose was measured at the day of scan (+7pi) in pigs 2, 3 and 4.

Supplementary Table 3. Alignment of diagnostic CT, diagnostic PET (^{18}F-FDG, ^{68}Ga-citrate, ^{11}C-PK11195 and ^{11}C-methionine), diagnostic SPECT (^{99m}Tc-Nanocoll and ^{111}In-leucocytes), gross pathology and microbiology in the pelvic (hind) limbs and pelvic region seven days after inoculation with *S. aureus* in the right femoral artery of pigs 1, 2 and 4; significant lesions were only present in the right side as reported here

PIG 1	CT	PET	SPECT	Gross pathology	Microbiology[B]
Soft tissue related to inoculation site	Subcutaneous located swelling, 5.2 x 5.2 x 2.0 cm	---	---[A]	Subcutaneous cystic lesion, diameter app. 5 cm	NT[C]
	---[A]	^{18}F-FDG: intramuscular, craniomedial thigh muscle region, 0.9 x 1.1 x 1.2 cm (metabolic measurement)	---	Abscess, craniomedial thigh muscle region, diameter approx. 1 cm	*S. aureus* (heavy growth), *Escherichia coli* (few colonies)[D]
Bones	Osteolysis (medulla) and sequestration, femoral head and neck	^{18}F-FDG: femoral head and neck	---	Suppurative osteomyelitis, femoral head and neck	NT
	Osteolysis (medulla and cortex) and sequestration, distal physis region femur	^{18}F-FDG: distal physis region femur	^{111}In-leukocytes: distal physis region femur	Suppurative osteomyelitis, distal physis region femur	*S. aureus* (moderate growth)
	Osteolysis (medulla), proximal physis region tibia	^{18}F-FDG: proximal physis region tibia	---	---	NT
	Osteolysis (cortex), distal physis region tibia	---	^{111}In-leukocytes: distal physis region tiba	---	NT
	Osteolysis (medulla and cortex) and sequestration, distal physis region metatarsus III	^{18}F-FDG: distal physis region metatarsus III ^{11}C-methionine: distal physis region metatarsus III	^{111}In-leukocytes: distal physis region metatarsus III	Suppurative osteomyelitis and medial suppurative periostitis, distal physis region metatarsus III	NT
Soft tissue peripheral to bones	Edema peripheral to distal femur	---	---	---	NT
	Swelling peripheral to distal metatarsus III	^{18}F-FDG: distal metatarsus III ^{11}C-methionine: distal metatarsus III	^{111}In-leukocytes: distal metatarsus III	Subcutaneous abscess medial to distal metatarsus III, diameter 1.5 cm	*S. aureus* (heavy growth)
Joints	---	---	---	Serous arthritis knee joint	*Aerococcus viridans* (heavy growth)
Lymph nodes	Mammary lymph node slightly enlarged ---	^{11}C-methionine: mammary lymph node ---	--- ---[E]	--- Enlarged medial iliac lymph nodes	NT NT

PIG 2	CT	PET	SPECT	Gross pathology	Micobiology[B]
Soft tissue related to inoculation site	---[A]	---	---	---	NT[C]
Bones	Osteolysis (medulla an cortex), patella	---	^{111}In-leukocytes: cortical osteolytic region of paella [99m]TC-Nanocoll: absence of activity in medulla of patella	Suppurative osteomyelitis, patella	NT

Utility of SPECT and PET to diagnose infection in a porcine osteomyelitis model

	CT	PET	SPECT	Gross pathology	Microbiology
Soft tissue peripheral to bones	Swelling and edema peripheral to the knee joint	^{18}F-FDG: tissue peripheral to patella and bordering patella ^{68}Ga-citrate: tissue peripheral to patella and bordering patella ^{11}C-methionine: tissue peripheral to patella ^{11}C-PK11195: tissue peripheral to patella	^{111}In-leukocytes: tissue peripheral and in particular lateral to patella	Cellulitis peripheral to patella, diameter approx. 10 cm	*S. aureus* (few colonies)
	Edema in the soft tissues of the thigh and in the soft tissues of the lower limb and tarsal joint	---	---	Subcutaneous edema in the lower limb and around the tarsal joint	NT
	Edematous region with gas-bubbles deep in the caudal thigh muscles	---	^{111}In-leukocytes: tissue deep in the caudal thigh muscles	---	NT
Joints	---	---	---	Fibrino-suppurative arthritis knee joint	*S. aureus* (heavy growth)
Lymph nodes	---	^{18}F-FDG: medial iliac lymph node area[F] ^{68}Ga-citrate: medial iliac lymph node area[F]	---[E]	Enlarged medial iliac lymph nodes	NT
PIG 4[G]	**CT**	**PET**	**SPECT**	**Gross pathology**	**Microbiology[B]**
Soft tissue related to inoculation site	Subcutaneous located swelling, 8.0 x 6.6 x 6.1 cm	^{18}F-FDG: sphere-formed subcutaneous accumulation, 4,7 x 6,0 x 6,4 cm (metabolic measurement) ^{68}Ga-citrate: sphere-formed accumulation ^{11}C-methionine: sphere-formed accumulation	^{111}In-leukocytes: subcutaneous located swelling	Subcutaneous abscess, diameter approx. 8 cm; abscess, craniomedial thigh muscle region, communicating with the subcutaneous abscess by a fibrous stalk, diameter approx. 1 cm	*S. aureus* (heavy growth), both abscesses
Bones	Osteolysis (medulla and cortex), almost entire metatarsus II	^{18}F-FDG: entire metatarsus II ^{68}Ga-citrate: entire metatarsus II ^{11}C-methionine: entire metatarsus II	^{111}In-leukocytes: entire metatarsus II and associated soft tissue (not possible to distinguish the two tissue components)	Suppurative osteomyelitis and suppurative periostitis, entire metatarsus II	NT
Soft tissue peripheral to bones	Swelling peripheral to metatarsus II	^{18}F-FDG: sphere formed accumulation, 2.6 x 4.6 x 5.1 cm (metabolic measurement) ^{68}Ga-citrate: semi-sphere formed accumulation located in the deep part ^{11}C-methionine: semi-sphere formed accumulation located in the deep part	^{111}In-leukocytes: soft tissue peripheral to metatarsus I	Subcutaneous abscess medial to metatarsus II, diameter 2,0 cm	*S. aureus* (heavy growth)
Joints	---	---	---	Arthritis joint between metatarsus II and proximal phalanx	NT
Lymph nodes	Mammary lymph node enlarged	^{18}F-FDG: mammary lymph node ^{68}Ga-citrate: mammary lymph node ^{11}C-methionine: mammary lymph node ^{11}C-PK11195: mammary lymph node	---	---	NT
	Medial iliac lymph node area slightly enlarged[F]	^{18}F-FDG: medial iliac lymph node area[F]	---[E]	Enlarged medial iliac lymph nodes	NT

[A]--- indicates absence of signal at any location within the stated tissue compartment. [B]All *S. aureus* isolates form the pigs were phenotypically indistinguishable from the inoculated strain. [C]NT indicates not tested. [D]Deemed to be a contaminant. [E]Only mammary lymph nodes scanned, i.e. included in the SPECT bed position. [F]Distinguishing the various anatomical soft tissue structures within the pelvic cavity by CT can be challenging, which is why the scan signal has been assigned to the area of the medial iliac lymph nodes. [G]Pig 3 was without infection and is not included in this table.

References

[1]   Soerensen KE, Nielsen OL, Jensen HE, Leifsson PS and Iburg TM. Pulmonary Lesions Following Intravenous Inoculation with A High Concentration of Staphylococcus Aureus in Pigs. Journal of Comparative Pathology 2010; 143: 324-324.

[2]   Leifsson PS, Iburg T, Jensen HE, Agerholm JS, Kjelgaard-Hansen M, Wiinberg B, Heegaard PM, Astrup LB, Olsson AE, Skov MG, Aalbaek B and Nielsen OL. Intravenous inoculation of Staphylococcus aureus in pigs induces severe sepsis as indicated by increased hypercoagulability and hepatic dysfunction. FEMS Microbiol Lett 2010; 309: 208-216.